NASA TECHNICAL NOTE

NASA TN D-5195

C. 1

NASA TN D-5195

CREEP-RUPTURE DATA FOR WELDED N-155 TUBES

by Richard E. Morris

Lewis Research Center

Cleveland, Ohio

NATIONAL AERONAUTICS AND SPACE ADMINISTRATION • WASHINGTON, D. C. • MAY 1969

CREEP-RUPTURE DATA FOR WELDED N-155 TUBES

By Richard E. Morris

Lewis Research Center
Cleveland, Ohio

NATIONAL AERONAUTICS AND SPACE ADMINISTRATION

For sale by the Clearinghouse for Federal Scientific and Technical Information
Springfield, Virginia 22151 – CFSTI price $3.00

ABSTRACT

Creep rupture pressure tests were conducted to obtain creep deformation and lifetime data for use in the design of a helium-to-air heat exchanger with a 10 000 hour life for nuclear airplane application. Design curves are presented for 2 percent strain, 5 percent strain, and rupture in a graph of stress against Larson-Miller parameter. Creep strength of tubes was about 2/3 of sheet strengths given in handbooks. Tube strength was limited by the strength of the weld. Thermally cycled specimens had approximately 10 percent lower strength and higher average equivalent bore strains than specimens tested at constant temperature.

CREEP-RUPTURE DATA FOR WELDED N-155 TUBES

by Richard E. Morris

Lewis Research Center

SUMMARY

This report covers the testing and analysis of data obtained from long time creep rupture tests of welded and drawn alloy N-155 (Iron Base 20Co-20Cr-20Ni-3Mo-2.5W-1Ta/Cb Superalloy) tube specimens. This alloy is a candidate material for a high temperature, high pressure, helium-to-air heat exchanger with a service life of 10 000 hours for nuclear airplane application.

Test data was obtained from tube specimens pressurized internally with helium, and exposed to high temperatures in air for long times. Test temperatures ranged from 1450° to 1780° F (1061 to 1244 K). Test times varied from 60 to 1857 hours. Helium pressures varied from 450 to 1800 psi (3.10 to 12.41 MN/m^2). Effective stresses at the inside radii of tubes tested varied from 2.35 to 11.25 KSI (16.2 to 77.6 MN/m^2). Commercially fabricated welded N-155 tubes tested had diameter-to-wall-thickness (D/w) ratios of 5.2 and 15. Most specimens were tested under conditions of constant temperature and pressure. The remainder were given daily thermal cycles with constant pressure.

Analysis of test data showed that the creep rupture strength of welded N-155 tubes was approximately two-thirds of the corresponding strength of N-155 sheet as given in handbook data. A graph of equivalent stress against the Larson-Miller parameter was found to correlate with experimental data. This graph can be used to predict the creep rupture life-times of welded N-155 tubes for conditions of temperature and equivalent bore stress over the ranges of temperatures, stress, lifetimes, and D/w ratios covered in these tests.

The weld zone of the tube wall was observed to be weaker than the parent metal. All tubes failed in the weld area. Tubes thermally cycled under constant internal pressure had approximately 10 percent lower creep rupture strength than tubes tested with constant temperature.

Thus creep rupture strengths of N-155 tubing could be improved by metallurgically strengthening the weld area or by the production of seamless tubing.

INTRODUCTION

Information on the strength of superalloy tubing was needed for preliminary design of a minimum weight, high temperature, high pressure, helium to air heat exchanger. For nuclear airplane application (ref. 1) this heat exchanger will be required to have a 10 000 hour lifetime with maximum reliability. No information on the creep deformation and rupture of tubing was available at the temperature and stress conditions of interest.

Handbook data on the tensile creep deformation and rupture of superalloys in the form of sheet or bars was generally available. Strength levels given for materials in these forms suggested that tube strengths required for the heat exchanger could be obtained.

Other investigators have used tensile test data in the analysis of creep deformation in internally pressurized cylinders. This approach assumes that tensile test (uniaxial stress) data can be related to the complex stress-strain behavior of potentially anistropic material in commercially manufactured tube form.

Finnie (ref. 2) pointed out that "the results of high-temperature creep tests on tubes loaded by torsion and by internal pressure cannot be explained by any of the methods of strain prediction given in the literature." The work of Zaslawsky (ref. 3) also showed that uniaxial test data was not sufficient to predict biaxial behavior. Chitty and Duval (ref. 4) showed that the ranking of alloys (ordered on the basis of strength) changed as the times under test were increased.

Creep deformation and rupture data from internally pressurized tubes was needed in order to avoid uncertainties in the prediction of creep deformation and rupture lifetimes based on tensile test data. To minimize the number of tube tests, a method of analysis was needed to provide design information over a complete range of temperatures, stresses, and lifetimes.

A stress-parameter graphical presentation of experimental data was selected for correlation of test data. Manson (ref. 5) discussed parametric methods for the presentation of tensile test data. Chitty and Duval (ref. 4) presented experimental creep rupture data for tubes using a parametric method. Other investigators have presented tube data in the form of isothermal plots of creep rupture stress against time to rupture. Reference 6 by McCoy and Weir is an example of the isothermal plot method.

The analysis selected for this paper was that of Bailey (ref. 7). He assumed the von Mises criterion to hold for creep strain and that the secondary creep rate could be represented by a power function of stress. Both assumptions were suggested as providing reliable predictions by Tagart (ref. 8) and Marin (ref. 9). Marin also indicated that for long lifetimes the primary creep strain is small compared to the secondary creep strain and hence the primary creep strain is often neglected.

N-155 is a member of the 20Co-20Ni-20Cr superalloy group. This alloy was selected as a candidate material for the heat exchanger because of its excellent strength at high temperature, weldability, fabricability, oxidation resistance, and metallurgical stability.

To simulate the service in the helium-to-air exchanger, tube specimens were internally pressurized with helium and heated to test temperature in air. Test temperatures and pressures were selected to obtain lifetimes in the neighborhood of 1000 hours. Time dependent factors such as metallurgical stability and oxidation may influence the creep strength of tubes. The long term tests permitted these factors to affect the experimental data.

The variation of properties of materials in different forms is an important part of the problem of predicting the creep rupture strength of tubes. These tests were conducted to obtain data from materials in the fabricated tube form under conditions approximately equivalent to proposed service conditions.

SYMBOLS

a inside radius, cm

B material constant

b outside radius, cm

D outside diameter, cm

P Larson-Miller Parameter

p pressure, MN/m^2

r radius, cm

T temperature, ^oF, ^oR

t time, hr

w wall thickness, cm

ϵ strain, cm/cm

$\dot{\epsilon}$ strain rate, cm/(cm-hr)

$\bar{\epsilon}$ equivalent strain, cm/cm

$\dot{\bar{\epsilon}}$ equivalent strain rate, cm/(cm-hr)

σ stress MN/m^2

$\bar{\sigma}$ equivalent stress, MN/m^2

Subscripts:

a inside radius

b outside radius

r radial

z axial

θ circumferential

Superscript

n material constant

PROCEDURES

Material

Tubing tested and evaluated in this report was welded and drawn N-155 (refs. 10 and 11), a member of the 20Co-20Cr-20Ni superalloy group. This alloy has been widely used in aircraft and other high temperature applications. This essentially austenitic alloy is recommended for service to 1500° F (1089 K) with relatively high stress. It can also sustain moderate stresses to 2000° F (1367 K).

This material has excellent oxidation resistance, good ductility, fabricability, and metallurgical stability in high temperature applications. It is available in all forms except seamless tubing.

Aeronautical Material Specification (AMS) 5585 dated October 1, 1960, lists specifications that apply to welded tubing manufactured from this alloy. Tubing was roll formed, welded, and drawn to size with intermediate anneals. Tubing received a final solution heat treatment at 2150° F ± 20 (1450 K ± 11) in a hydrogen atmosphere followed by furnace cooling at a rate approximately equivalent to air cooling. Two different sizes of tubing were fabricated. Each was fabricated from a different heat of alloy by the same manufacturer. The tubing was ultrasonically inspected for internal flaws, inspected for external flaws with fluorescent penetrant, and was found to be crack free.

Tube sizes, heats, and chemical analyses of alloys are given in table I. The weight percentages of constituents were within the tolerance limits established in AMS 5585. No significant change in composition occurred during the long time tests of specimens analyzed.

TABLE I. - CHEMICAL COMPOSITION OF N-155[a] SPECIMENS

Specimen size				Heat	Sample	Carbon	Manganese	Silicon	Phosphorus	Sulfur	Chromium	Nickel	Molybdenum	Cobalt	Columbium or tantalum	Tungsten	Nitrogen
Diameter		Wall thickness				Composition, wt %											
in.	cm	in.	cm														
-----	-----	-----	-----	------	AMS 5585	0.08 - 0.16	1.00 - 2.00	[b]1.00	[b]0.030	[b]0.030	20.0 - 22.50	19.00 - 21.00	2.50 - 3.50	18.50 - 21.0	0.75 - 1.25	2.00 - 3.00	0.10 - 0.20
0.375	0.953	0.025	0.064	C-3110	As-received	0.14	1.65	0.60	0.015	0.003	21.02	20.04	3.01	19.13	1.20	2.64	0.11
					7 after test	0.13	1.67	0.65	0.016	0.009	21.04	19.91	3.03	19.15	1.24	2.88	0.15
0.250	0.635	0.048	0.122	C-4836	As-received	0.09	1.43	0.42	0.013	0.006	21.27	19.62	3.00	19.66	0.98	2.48	0.17
					24 after test	0.10	1.63	0.49	0.015	0.010	20.54	19.75	2.97	19.63	1.12	2.65	0.15

[a]Iron base alloy.
[b]Maximum.

Specimens

N-155 tube specimens 15 inches (38.1 cm) long were fabricated with gas tungsten-arc welds as shown in figure 1. The length was selected so that the welded connection to a stainless steel Type 304 inlet tube on the other end were outside of the high temperature region of the 12-inch long resistance furnaces used for the tests.

The two sizes of tubes tested were 0.635 centimeter diameter by 0.122 centimeter wall and 0.953 centimeter diameter by 0.064 centimeter wall. The tubes had diameter

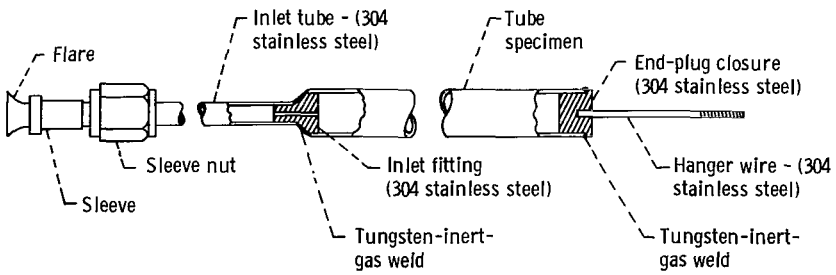

Figure 1. - N-155 tube test specimen.

to wall thickness ratios (D/w) of 5.2 and 15.0, respectively. Both tube sizes are classified as thick tubes.

Materials for specimens were ultrasonically cleaned and degreased to remove lubricants and foreign matter from all surfaces. The end plug closure and the stainless steel inlet tube were then welded in place. Completed specimens were inspected with a mass spectrometer to assure that all welds were helium leak tight.

Tests

The tube test rig is shown schematically in figure 2. Four creep rupture pressure test specimens were tested at a time in an electric resistance furnace. The majority of specimens were tested at constant temperature and static internal helium pressure to failure. Furnace temperature was measured and recorded using chromel-alumel thermocouples located at each end and in the middle of a 4-inch (10.2-cm) long temperature-flattened (constant temperature $\pm$ 1.7 K) zone. Pressure transducers in each specimen pressure circuit were used to monitor and to provide a continuous record of specimen pressures.

Twelve specimens were thermally cycled once per day from test temperature down

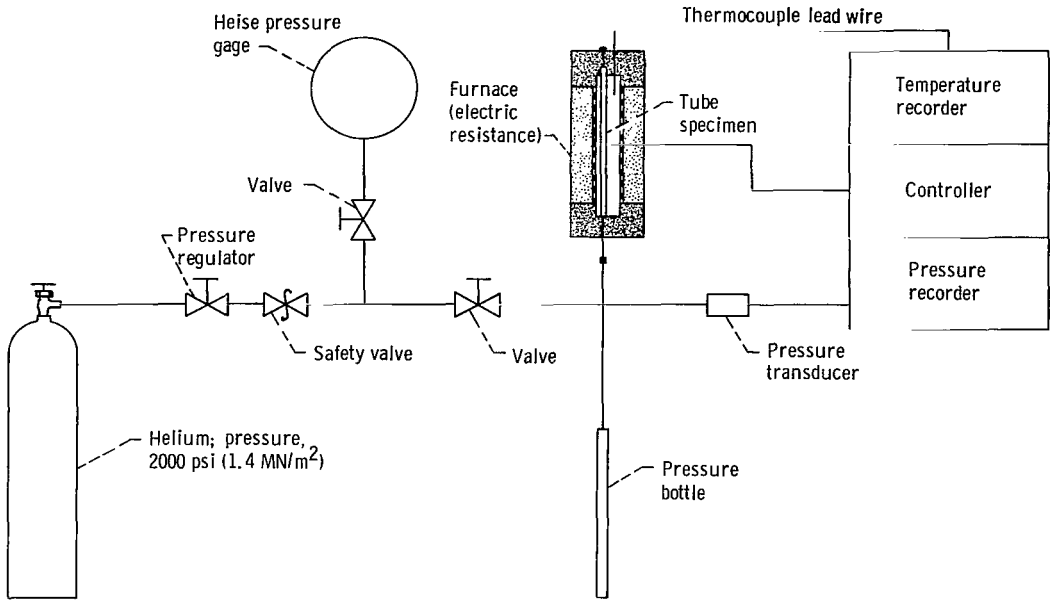

Figure 2. - Heat exchanger tube test rig. Maximum test temperature, 1800° F (1255 K); maximum test pressure, 1800 psi (12.41 MN/m^2).

to 400° F (478 K) and back to test temperature, 5 days per week to failure. Otherwise, the specimens were held at test temperature. Cooling the furnace was accomplished by blowing air through the furnace to lower the temperature to 400° F (478 K) in a period of about 20 minutes. Specimens were kept at about 400° F for 3 hours. Return to test temperature required about 30 minutes. The time for each cooling cycle was set at 4 hours.

Test temperatures had a range of 1450° to 1780° F (1061 to 1244 K). Test pressures varied from 450 to 1800 psi (3.1 to 12.4 MN/m^2). Effective stresses at the inside radii of tubes tested varied from 2.35 to 11.25 ksi (16.2 to 77.6 MN/m^2). Long term tests were run to determine the potentially damaging effects of oxidation and metallurgical changes. Test times for this series of tests varied from 60 to 1857 hours.

Metallography

Photomicrographs were made of the tube material before and after testing. Sections of tubes were taken on planes perpendicular to the axis of the tube specimens. Sections of failed tubes were taken through the tube fracture close to the point of failure. Principal creep strains occurred in the planes of the sections. Sections were prepared with an electrolytic chromic acid etch.

Accuracy

The furnace controller used in these tests had a sensitivity of ±2 microvolts. Thermocouples and other sources of variation caused the uncertainty of specimen temperature to be approximately $\pm 5^{\circ}$ F (±2.8 K). Pressure uniformity was affected by the presence of small leaks in pressurized specimen circuits and the expansion of the specimen during creep deformation. Overall pressure accuracy is estimated ±10 psi (±0.07 MN/m^2) for all specimens. Specimens were fabricated from tubing manufactured with a tolerance on wall thickness of ±10 percent.

Analysis

The solution of the plasticity problem of a tube with internal pressure undergoing creep deformation was presented by Bailey (ref. 7). The assumptions involved in his solution as discussed by Johnson and Mellor (ref. 12) appear to be justifiable for tube behavior observed in this testing program. Bailey's equations for stress and strain-rate distribution are used in the analysis of the data presented in this report.

The parametric method of presentation of stress-rupture is often used with tensile data. Chitty and Duval (ref. 4) used the parametric method to present creep-rupture data for tubes. They, however, used mean stress to characterize the wall stress. The mean wall stress is not associated with a stress-strain-rate distribution. This analysis utilizes the parametric method of presentation in conjunction with the Bailey equations for the stress and strain-rate distribution in the tube wall undergoing uniform creep.

Here it is assumed that the creep strain-rate is uniform from initial loading to final rupture of the specimen. In the usual tensile test, little engineering attention is given to various stages of creep. Primary creep being a relatively small part of long term creep is often neglected. Tertiary creep is associated with instability or impending failure. The stage of most general engineering interest is therefore secondary creep. In practice the rupture lifetime will be avoided by application of a safety factor with the result that lifetime stress levels associated with low creep rates do not exceed the secondary creep rate. Tubes tested for long lifetimes under conditions of high temperature creep-rupture with a limited volume of high temperature, high pressure gas tend to form very small radial cracks through the tube wall and lose pressure. There is a question as to whether tertiary creep or instability deformation occurs in tubes subjected to high temperature service for long lifetimes. For the purposes of this analysis the assumption of uniform creep-rate for the life of the tube appears to be reasonable.

Experimental test data was analyzed with the computer code of Mendelson, Roberts, and Manson (ref. 13) to optimize the time-temperature parameter for N-155. The code selects the parameter and parameter constants to provide the smallest standard deviation.

Assumptions

In the analysis of creep deformation of a tube deforming under a uniform deformation rate, certain assumptions are required.

(1) A greatly simplifying assumption for purposes of analysis is that the material is isotropic.

(2) The von Mises criterion for yielding of the tube wall is applicable to creep in pressure tubes.

(3) The principal strain rates are proportional to the reduced or deviatoric principal stresses.

(4) The principal axes of stress and creep strain rate are coincident and remain so during strain up to moderate amounts.

(5) The axial strain-rate is zero. Experimental data obtained by others verifies that this assumption is reasonable; that is, the axial strain rate is experimentally very small.

(6) The exponential stress-strain rate law of Norton and Bailey (ref. 14) is applicable.

$$\dot{\epsilon} = B\bar{\sigma}^n \tag{1}$$

A number of investigators have verified that this relation holds for several materials, especially for low stresses.

(7) Strain rate $\dot{\epsilon}_{\theta b}$ is equal to the strain measured on the outside diameter at rupture divided by the lifetime of the specimen. That is, the strain rate is assumed to be uniform for the life of the specimen.

Stress-Strain Distribution

With these assumptions the stresses in the tube will be given as follows:

$$\sigma_r = -\frac{\left(\frac{b}{r}\right)^{2/n} - 1}{\left(\frac{b}{a}\right)^{2/n} - 1} p \tag{2}$$

$$\sigma_\theta = \frac{1 - \left(\frac{n-2}{n}\right)\left(\frac{b}{r}\right)^{2/n}}{\left(\frac{b}{a}\right)^{2/n} - 1} p \tag{3}$$

$$\sigma_z = \frac{1 - \left(\frac{n-1}{n}\right)\left(\frac{b}{r}\right)^{2/n}}{\left(\frac{b}{a}\right)^{2/n}} p \tag{4}$$

$$\bar{\sigma} = \frac{\frac{\sqrt{3}}{n}\left(\frac{b}{r}\right)^{2/n}}{\left(\frac{b}{a}\right)^{2/n} - 1} p \tag{5}$$

Important strain relations required are:

$$\dot{\epsilon}_{\theta a} = \left(\frac{b}{a}\right)^2 \dot{\epsilon}_{\theta b} \tag{6}$$

$$\bar{\epsilon}_a = \frac{2\left(\frac{b}{a}\right)^2 \epsilon_{\theta b}}{\sqrt{3}} \tag{7}$$

The Bailey equations require a material constant n which is the stress exponent in equation (1). Conrad (ref. 15) found the stress exponent for N-155 to vary from 4 to 5 for stresses less than 15 ksi (103.4 MN/m^2) for temperatures from 1600 to 2000° F (1144 to 1478 K). The stress exponent n is temperature dependent so that equation (1) holds only for a limited range of temperature. The value used for n in this analysis is 4.5.

Relative values for the stresses in the plastically deforming tube can be examined by alternately substituting the inner radius a and the outer radius b for r in equations (2) to (5).

Equation (2) gives a compressive stress equal to the pressure at the inside radius a and drops to zero at the outside radius b.

The numerator in equation (3) for the hoop stress becomes 2/n at the outside

radius. For $r < b$, $\sigma_{\theta r} < \sigma_{\theta b}$. The minimum hoop stress occurs at the inside radius, $r = a$. For the case of $n = 4.5$, and $b/a > 3.75$, $\sigma_{\theta a}$ is a compressive stress.

The numerator in equation (4) becomes $1/n$ for $r = b$, and $\sigma_{zb} = 1/2\ \sigma_{\theta b}$. For $r < b$, $\sigma_{zr} < \sigma_{zb}$. The axial stress is a minimum at the bore of the tube. For $b/a \geq 1.76$, σ_{za} is a compressive stress.

Equation (5) gives the equivalent stress by the distortion energy theory. This equation gives a maximum equivalent stress at the bore of the tube, and a minimum value at the outside radius.

Thus, the stresses on the outside of the tube are biaxial tensile stresses. The hoop stress is the maximum direct stress in the tube wall, and the biaxial stresses are in the ratio of 2:1. The equivalent stress is a minimum at the outside radius.

At the bore of the tube, the equivalent stress is a maximum. The hoop stress, the axial stress and the radial stress have minimum values.

Strain Measurement

Circumferential strain at fracture was obtained by taking the ratio of the change in diameter of the failed specimen to the initial specimen diameter. Two measurements were made at each end of the crack as shown in figure 3. Tube diameters on which measurements were taken were perpendicular and at a circumferential angle of 45° with the axial line of the crack. Four measurements taken on each tube were averaged to obtain the strained diameter for the circumferential strain calculation. Measurement of the rupture diameter represented the expansion of the tube under test conditions. This method of measurement was used to avoid local deformations at the point of rupture.

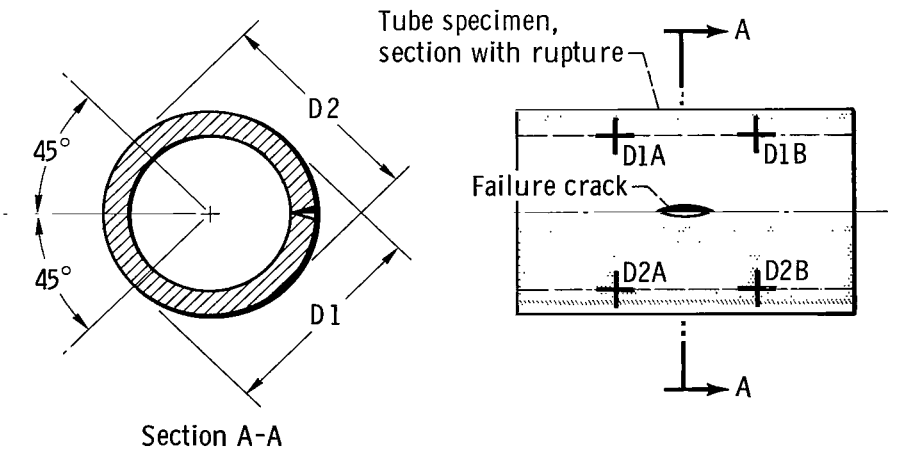

Figure 3. - Positions for post-test measurements of tube diameter for determination of fracture strain.

TABLE II. - WELDED N-155 TUBE DATA

Sample	Specimen size				Type of test	Temperature		Pressure		Equivalent stress		Lifetime, hr	Circumferential strain, $\epsilon_{\theta b}$, percent	Ultimate equivalent bore strain, $\bar{\epsilon}_a$, cm/cm	Equivalent bore strain rate, $\dot{\bar{\epsilon}}_a$, cm/cm-hr
	Diameter		Wall thickness												
	in.	cm	in.	cm		°F	K	psi	MN/m^2	ksi	MN/m^2				
1	0.375	0.953	0.025	0.064	Static	1600	1144	1100	7.61	6.88	47.4	410	5.85	0.090	219.0×10^6
2						1600	1144	1100	7.61	6.88	47.4	385	5.05	.077	201.0
3						1615	1152	800	5.52	5.00	34.5	1047	5.98	.092	87.5
4						↓	↓	↓	↓	↓	↓	1003	5.04	.078	77.3
5												1068	6.12	.094	87.7
6												1017	5.51	.085	83.1
7						1450	1061	1800	12.41	11.25	77.6	1857	5.38	.083	44.5
8						↓	↓	↓	↓	↓	↓	1762	6.70	.103	58.3
9												1793	----	-----	----------
10												1619	4.76	.073	45.1
11						1740	1222	450	3.10	2.81	19.4	420	4.87	.075	177.5
12						1617	1153	800	5.52	5.00	34.5	1060	4.21	.065	60.9
13								800	5.52	5.00	34.5	1094	6.32	.097	88.5
14								1100	7.58	6.88	47.4	280	8.02	.113	404.0
15								1100	7.58	6.88	47.4	282	5.40	.083	293.0
16						1725	1214	470	3.25	2.94	20.3	545	3.78	.058	106.0
17						↓	↓	470	3.25	2.94	20.3	581	6.65	.102	175.0
18								717	4.94	4.48	30.9	140	3.89	.060	424.0
19								717	4.94	4.48	30.9	147	5.61	.086	584.0
20	.250	.635	.048	.122		1660	1178	1800	12.41	3.58	24.7	1223	2.78	.084	74.2
21												1137	2.79	.084	68.7
22												1121	2.75	.083	74.2
23												1246	2.67	.081	64.8
24						1725	1214	1180	8.14	2.35	16.2	1470	----	-----	----------
25												1381	3.30	.100	72.4
26												1347	3.18	.096	71.5
27												1360	3.06	.093	68.1
28						1760	1234					590	3.38	.102	173.5
29												623	3.54	.107	172.0
30								1800	12.41	3.58	24.7	138	2.47	.075	540.0
31								1800	12.41	3.58	24.7	157	2.90	.088	559.0
32					Thermal	1780	1245	1180	8.14	2.35	16.2	272	4.35	.132	484.0
33					cycled			1180	8.14	2.35	16.2	266	3.30	.100	376.0
34								1800	12.41	3.58	24.7	60.5	2.42	.073	1210.0
35												63.2	3.14	.095	1500.0
36						1647	1171					1090	3.18	.096	88.4
37												1132	3.22	.097	86.1
38												1069	3.10	.094	87.8
39												1057	2.90	.088	83.1
40						1625	1160					1588	3.82	.116	72.8
41												1556	3.58	.108	69.7
42												1521	3.38	.102	67.3
43												1492	3.26	.099	66.1

Graphical Procedures

Stress, temperature, and lifetime data from table II were used to plot figure 4. The Larson-Miller parameter with the required constant, 17.2, was obtained with a computer code (ref. 13).

Circumferential strain measurements were converted into ultimate equivalent bore strains using equation (7). Equivalent strain rates were obtained from ultimate equivalent bore strains by dividing by the lifetimes in hours. The time to reach 2 or 5 percent

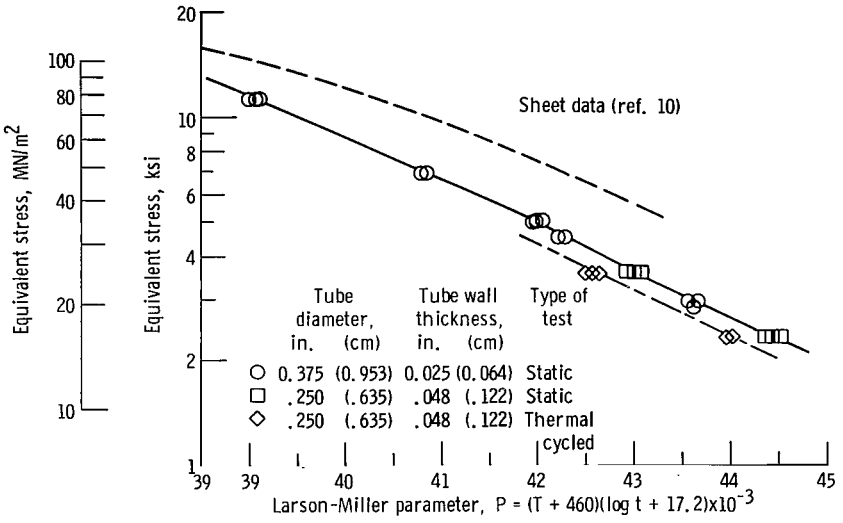

Figure 4. - Equivalent stress versus Larson-Miller parameter for creep rupture of welded N-155 tubes.

strain was based on the equivalent strain rate obtained for each specimen. Parametric plots of 2 and 5 percent strain data are shown in figure 5.

Circumferential strain measurements and ultimate equivalent bore strains for test specimens are listed in table II. A log-log plot of equivalent bore stress against equivalent bore strain-rate is given in figure 6.

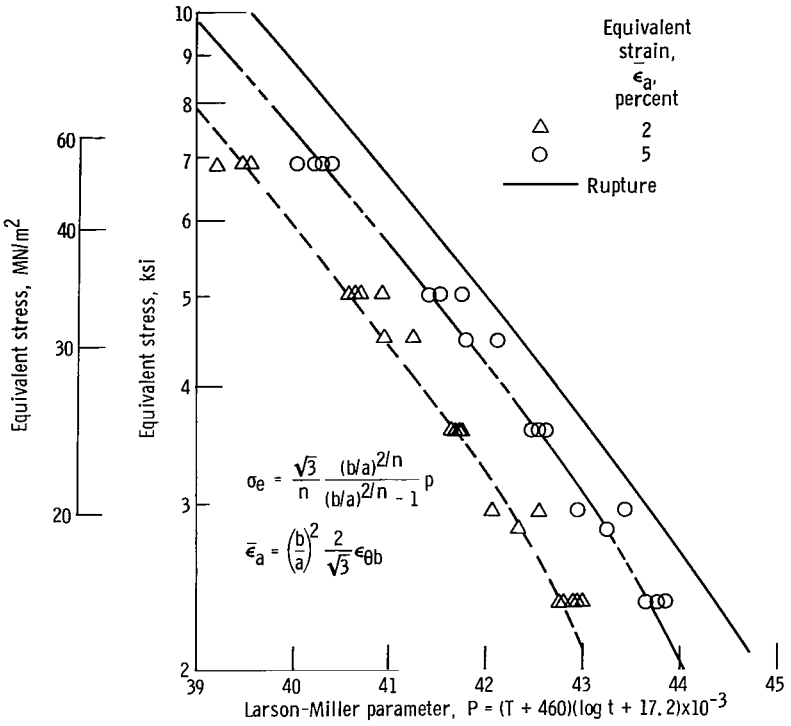

Figure 5. - Equivalent stress versus Larson-Miller parameter for welded N-155 tubes. (Stresses and strains are values in bores of tubes by plasticity solution of Bailey (ref. 7). Data for specimens tested at constant temperature and pressure.)

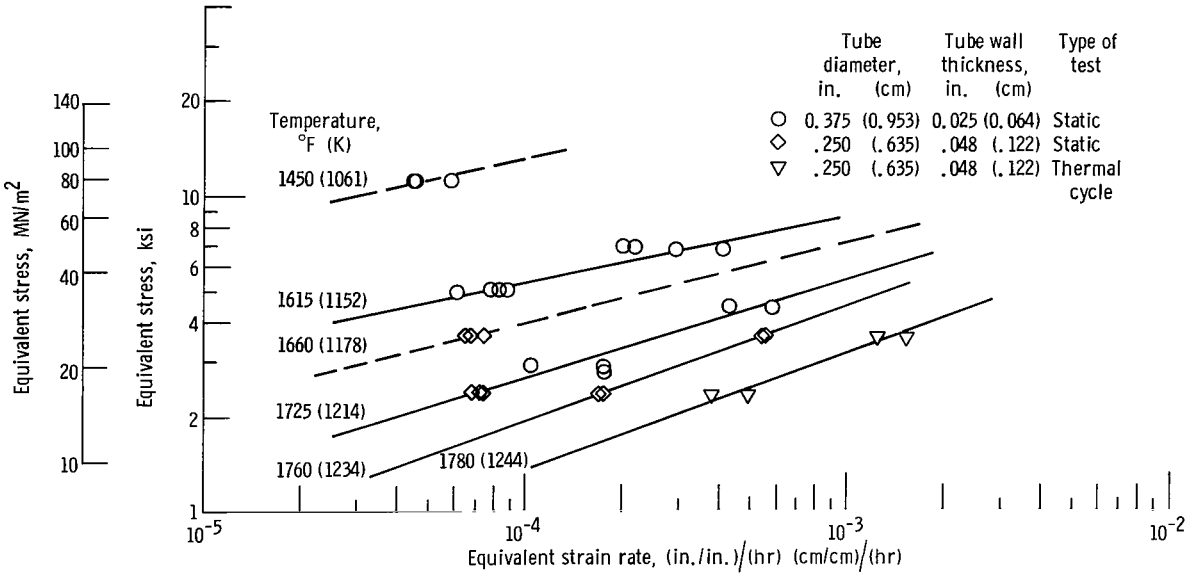

Figure 6. - Equivalent stress versus equivalent strain rate in bores of welded N-155 tubes.

RESULTS AND DISCUSSION

Thirty-one welded and drawn N-155 tube specimens were tested under conditions of constant helium internal pressure and constant temperature in an air atmosphere. Test temperatures ranged from 1450° to 1780° F (1061 to 1244 K). Helium test pressures varies from 450 to 1800 psi (3.1 to 12.4 MN/m^2). Effective stress at the inside radii of tubes tested varied from 2.35 to 11.25 ksi (16.2 to 77.6 MN/m^2).

Twelve specimens were thermally cycled once a day, five days a week, to failure with constant internal helium pressure. Thermal cycles involved forced air cooling the specimens in the furnace from test temperature down to 400° F (478 K) in a period of about 20 minutes, holding at 400° F (478 K), and then heating back to test temperature with normal furnace power. Heating to test temperature required about 30 minutes and the total cycle time was 4 hours. Test data from all specimens are listed in table II and plotted in figure 4.

As discussed under Materials, two heats of tubing were tested. The primary difference between the specimens from the two heats was the D/w ratio. One set were thick tubes with a D/w ratio of 5.2. The other set, also classed as thick tubes, were relatively thin-wall specimens with a D/w ratio of 15.

Correlation

Attempts to predict the creep rupture strengths of welded tubes on the basis of sheet data were unsuccessful. Experimental lifetimes at selected temperatures and stresses were much shorter than the predicted lifetimes. Reliable lifetime predictions were obtained using the Larson-Miller parametric method to correlate the experimental tube data.

Stresses and Larson-Miller parameter values are shown in the graph of figure 4 and table II. Stresses were calculated with equation (5) for an internally pressurized tube undergoing creep deformation at a uniform creep rate. The plotted stress is the maximum equivalent stress by the distortion energy theory at the inside surface of the tube specimen. The value for the stress exponent n used in these calculations was 4.5.

Stress, lifetime, and temperature data for tubes tested at constant temperature were used as input in the computer program of Mendelson, Roberts, and Manson (ref. 13) for the optimization of time-temperature parameters for creep and rupture. The program selected the Larson-Miller parameter as the parameter best correlating the data. The program also selected a value of 17.2 for the constant required for use with the parameter.

The standard deviation of the experimental data from the Larson-Miller curve fitted

to the data was 6.2 percent based on the prediction of the lifetime at a given stress and temperature condition.

Experimental tube strengths were generally about two-thirds of the strengths shown for tensile creep rupture tests of sheet specimens. The ratio was somewhat greater at higher stress levels.

Data for thermally cycled specimens are plotted in figure 4 and listed in table II. Cycled specimens had approximately 10 percent lower creep rupture strengths than specimens tested at constant temperature. Equivalent strain rates and ultimate equivalent bore strains were greater for all cycled specimens than for specimens tested at constant temperature.

Metallography

Figures 7 and 8 are photographs of tube failures in the two different sizes of tubes tested. All specimens failed in the weld area and there was no visible difference between the failures in thermally cycled specimens and failures in specimens tested at constant temperature.

Figures 9 and 10 show structure of the 3/8-inch (0.953-cm) diameter tubing as furnished by the manufacturer. The cast structure of the weld area shows carbide phases. The parent metal shows more complete phase solution. The matrix and grain boundaries are relatively clean; the carbides are few and are randomly distributed.

Figures 11 to 13 show the structure of the tube wall near the failure in specimen 24. This tube was exposed to 1725° F (1214 K) for 1470 hours. The weld metal shows appreciably smaller grain size compared to the parent metal. The parent metal has changed showing some grain growth, appreciable grain boundary segregation, and depletion of second phase particles.

Figures 14 to 16 show the structure of the tube wall near the failure in specimen 7. This tube was exposed to 1450° F (1061 K) for 1857 hours. This structure shows no grain growth, less grain boundary carbide precipitation, and no appreciable particle depletion. There is also less oxidation indicated, and less alloy depletion at the surface as compared to the specimen run at 1725° F (1214 K). Figure 13 shows that the 1450° F (1061 K) specimen failure was a much more local failure than the 1725° F (1214 K) specimen failure shown in figure 11.

Sigma phase, a hard, brittle, intermetallic compound, forms most rapidly in iron-chromium alloys in the temperature range of 1600° to 1650° F (1144 to 1172 K). Formation of this phase is associated with embrittlement.

Woodyatt, et al (ref. 16) presented a procedure for the prediction of intermetallic phase occurrence from compositions of superalloys using electron vacancy numbers. Electron vacancy numbers calculated for the 2 heats of N-155 alloy given in table I indi-

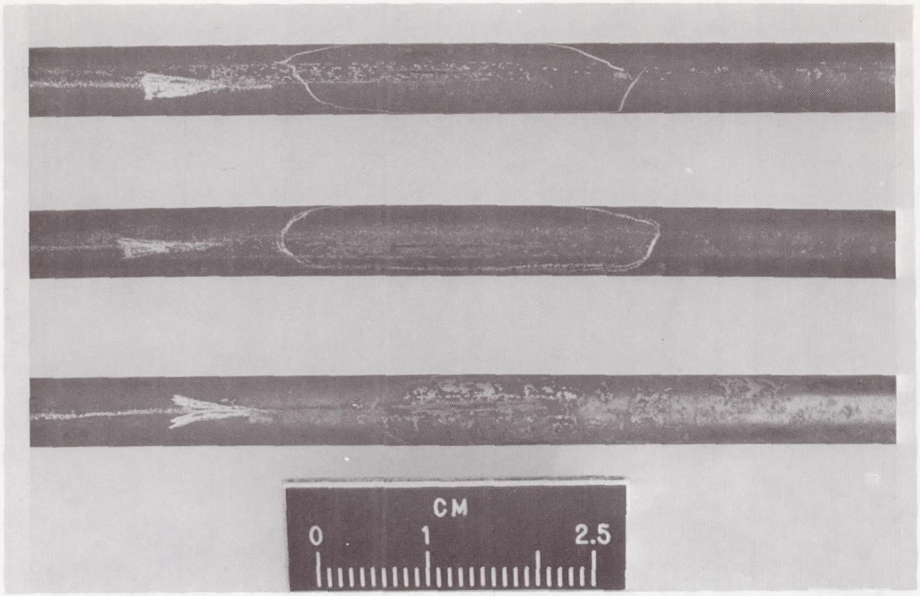

C-68-940

Figure 7. - Ruptures in 0.250-inch (0.635-cm) diameter by 0.048-inch (0.122-cm) wall N-155 tubes.

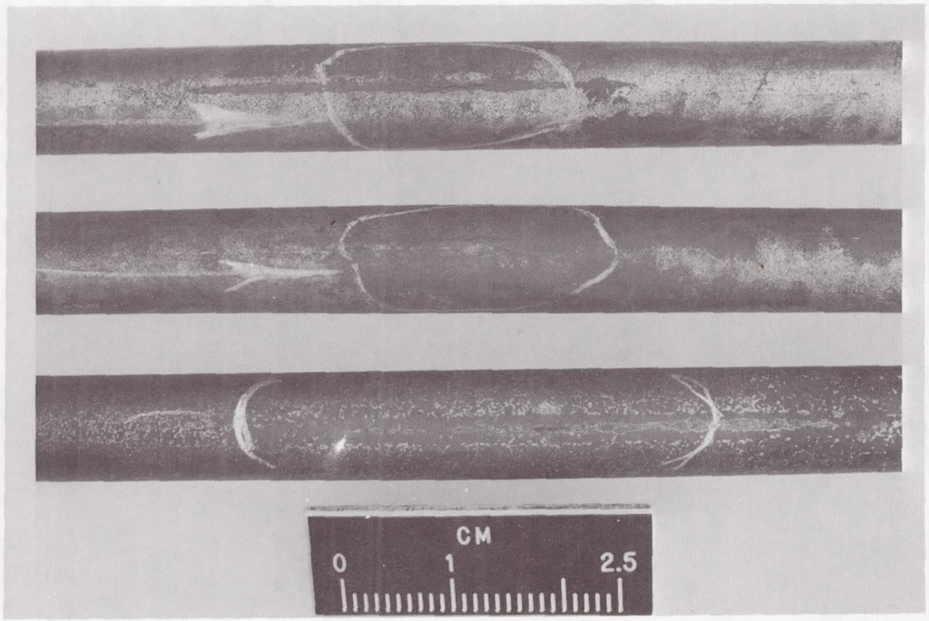

C-68-941

Figure 8. - Ruptures in 0.375-inch (0.953-cm) diameter by 0.025-inch (0.064-cm) wall N-155 tubes.

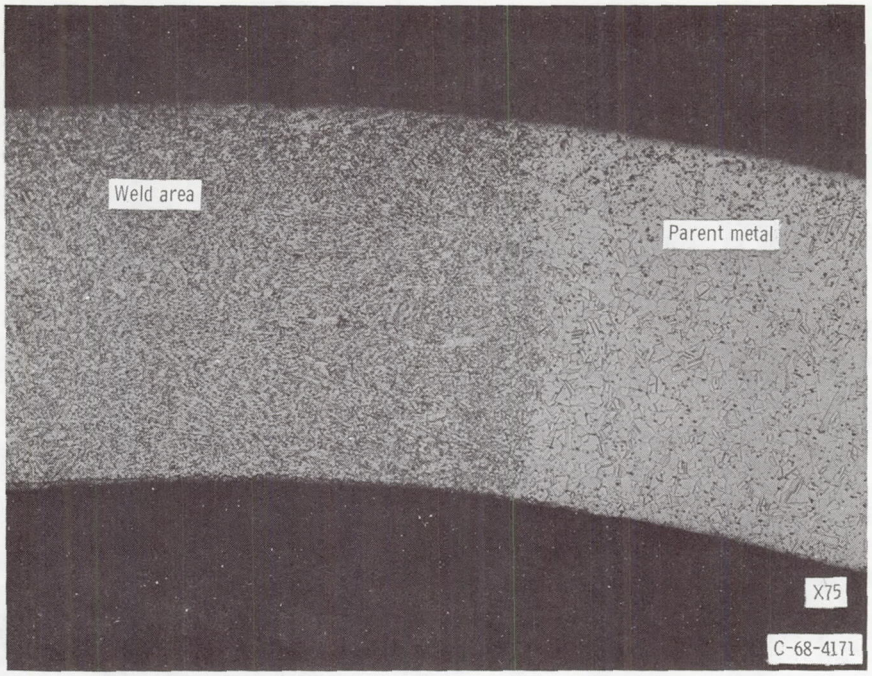

Figure 9. - 0.375-Inch (0.953-cm) diameter by 0.025-inch (0.064-cm) wall tube section; as received.

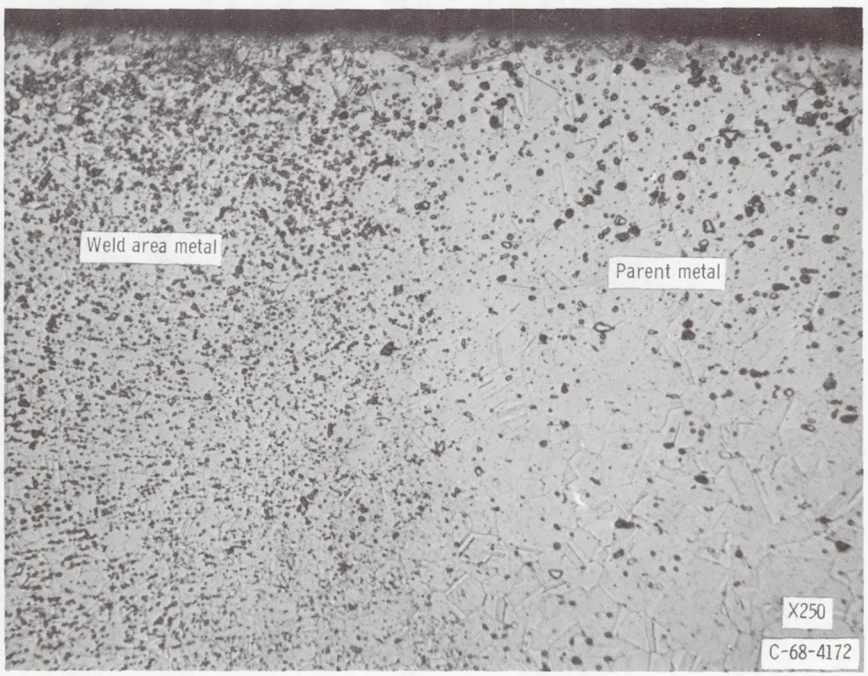

Figure 10. - 0.375-Inch (0.953-cm) diameter by 0.025-inch (0.064-cm) wall tube section; as received. Structural detail of parent and weld areas.

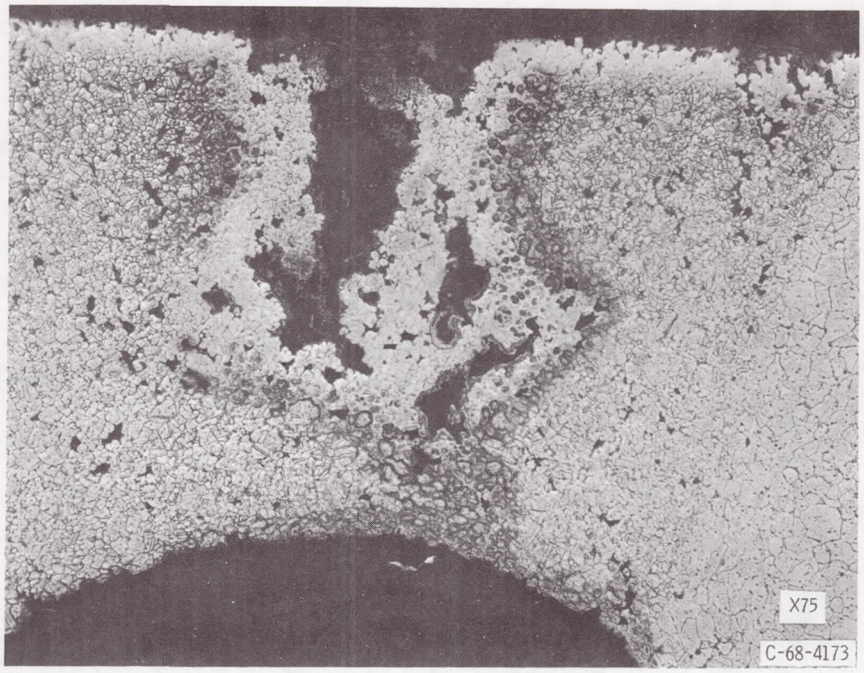

Figure 11. - Failure in weld area after 1470 hours at 1725° F (1214 K). Specimen 24.

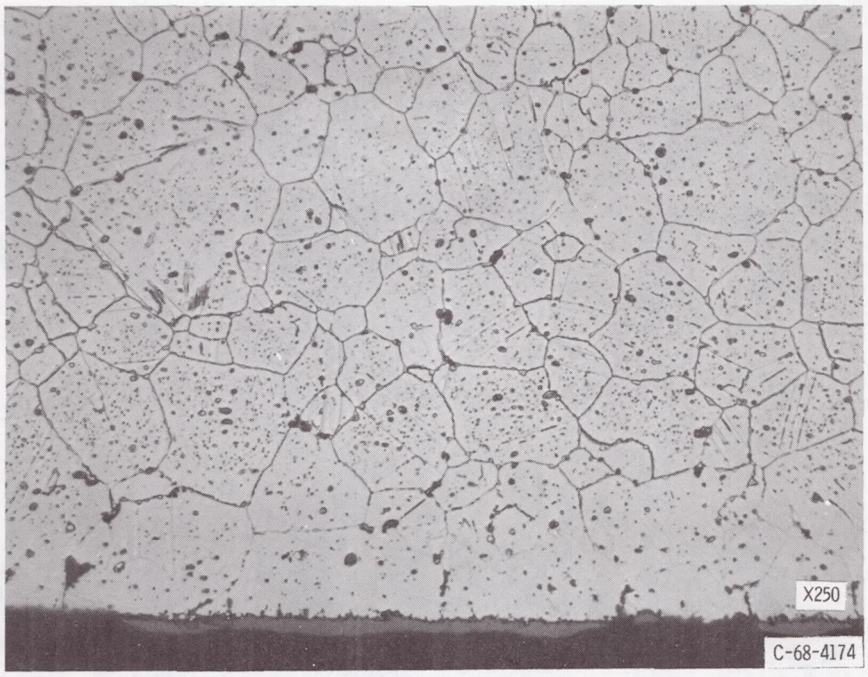

Figure 12. - Structural detail of parent metal after test. Specimen 24.

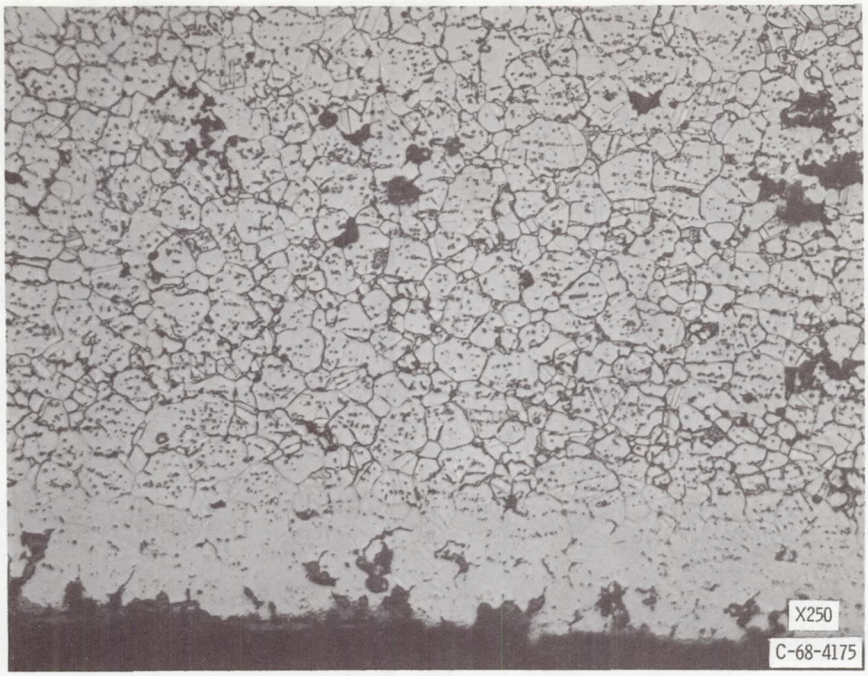

Figure 13. - Structural detail of weld zone after test. Specimen 24.

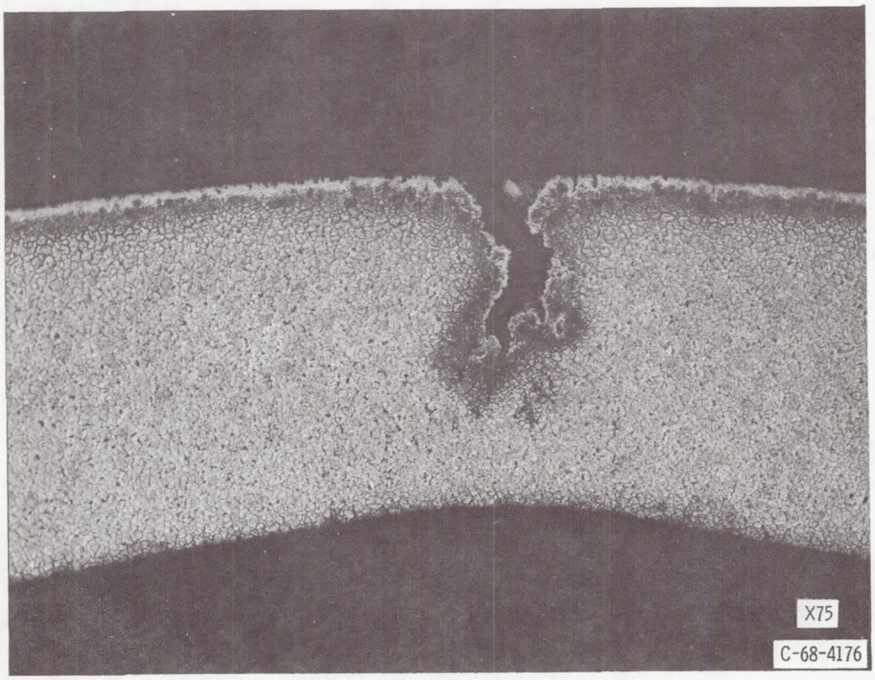

Figure 14. - Failure in weld area after 1857 hours at 1450° F (1061 K). Specimen 7.

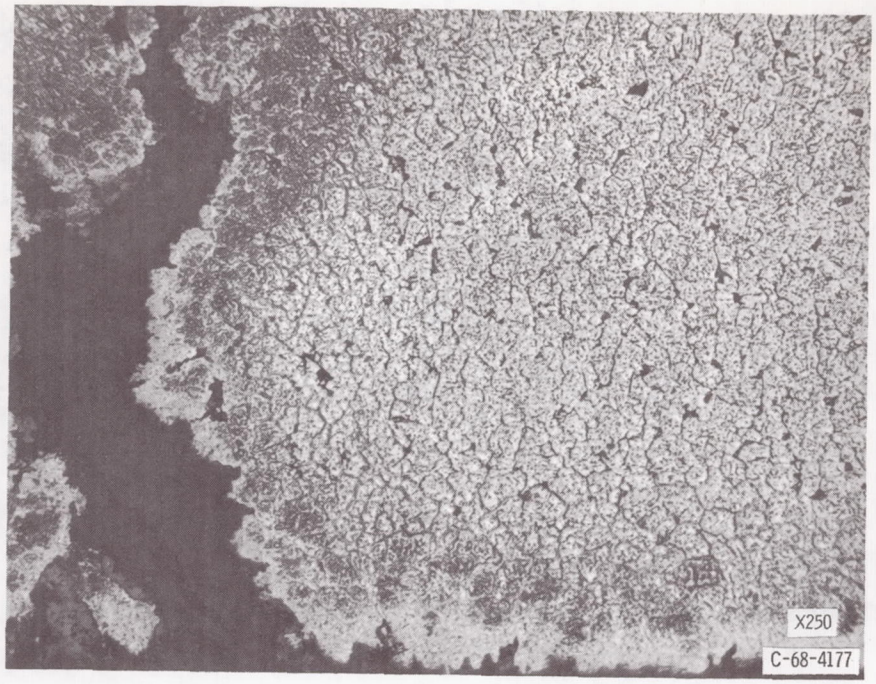

Figure 15. - Structural detail in weld area after test. Specimen 7.

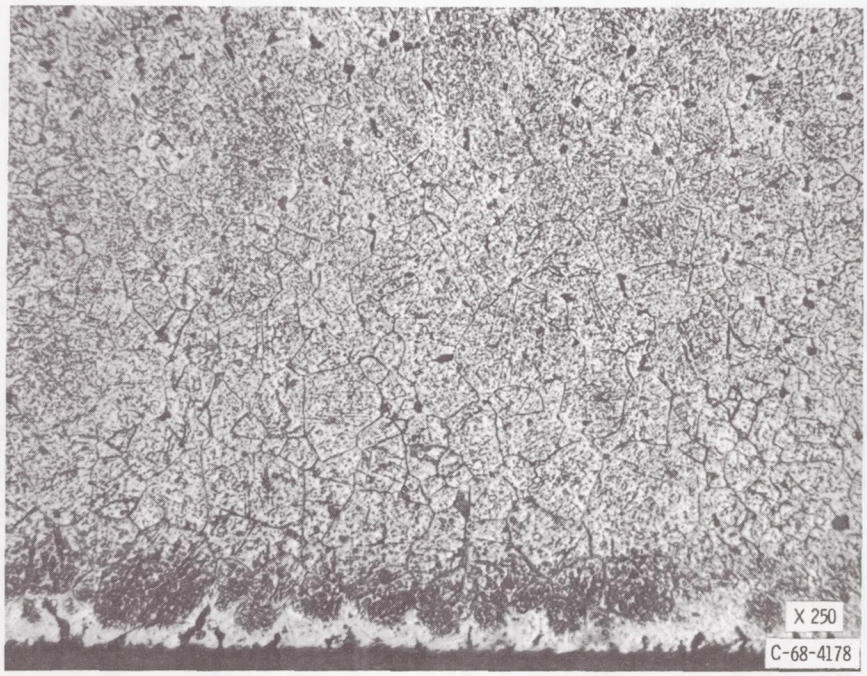

Figure 16. - Structural detail in parent metal after test. Specimen 7.

cate that this alloy may be instability prone. The formation of carbide and/or intermetallic phases may embrittle the structures.

Weld Zone Weakness

Welded N-155 tube specimens tested had low creep rupture pressure strengths compared to published tensile data. The maximum equivalent stress by the distortion energy heory is located in the bore of the tube and is given by equation (5) for r = a. Figure 4 (p. 13) shows that the equivalent stress-parameter data for tubes falls below the stress-parameter data for tubes falls below the stress-parameter graph of uniaxial tensile data. Tube strengths were generally about two-thirds of the strengths shown for tensile creep rupture tests of sheet specimens. The ratio was somewhat greater at higher stress levels.

Carbide phases identify the weld zone of the tube wall as received as shown in figures 9 and 10. All specimens tested failed in the weld area of the tube wall. Creep strain occurred preferentially in the weld material as shown in figures 11 and 14. The weld zone of the tube wall was visible as a line parallel to the axis of the tube on failed specimens because of the high strain in thr weld area (figs. 7 and 8).

The creep rupture strength of tubes was limited by the strength of the alloy in the weld area of the tubes. Tube strength can be improved by metallurgically increasing the strength and creep resistance of the alloy in the weld area of the tube wall. The production of seamless tubing would eliminate the problem of the weld.

Fracture

Fracture initiated in the weld area and at the outside surface of all tube specimens tested. Oxidation reduced the strength of the metal at the outside surface. Fractures occurred on essentially radial planes parallel to the axis of the tube.

The stress distribution in a tube undergoing uniform creep deformation supports the fracture behavior observed experimentally.

(1) The axial stress at the outside surface is equal to 1/2 the circumferential tensile stress. These biaxial tensile stresses are associated with reduced fracture strains compared to the uniaxial tensile case (ref. 3).

(2) The circumferential tensile stress at the outside surface is the maximum principal stress in the tube. This stress is greater than the distortion energy equivalent stress for this position.

(3) The maximum equivalent stress by the distortion energy theory is at the inside radius of the tube. Higher distortion energy equivalent stresses are associated with

more ductile behavior. Principal tensile stresses have minimum values in this location.

Thus, fracture initiated at the outside of surface of the specimen in material weakened by oxidation. The circumferential stress was a maximum in a stress field associated with reduced ductility.

Creep Strain Rate

As explained in assumption (7) and under Strain Measurement, creep strain rate was obtained by taking the strain at rupture divided by the lifetime of the tube. Thus, creep strain rates listed in table II are average values based on the assumption that creep strain rates were uniform over the lifetimes of the specimens.

Figure 6 (p. 14) is a log-log plot of equivalent bore stress against equivalent bore strain rate. The equivalent strain rate increased more rapidly with increased stress at 1615° F (1153 K) than at 1760° F (1233 K). The slopes of the isothermal lines are approximate values for n in equation (1). The n-values are approximate because the plotted average equivalent stresses were calculated using the assumed value of $n = 4.5$.

The expected behavior of stress against creep strain rate data with increasing temperatures would be a change in the slopes of the isothermal lines corresponding with increasing values for n. The change in slopes with increasing temperature in figure 3 represents decreasing values of n. This contrary behavior of the slopes of the isothermal lines in this graph could indicate that a metallurgical change occurred in the specimens at higher temperatures resulting in increased resistance to creep at higher temperatures.

The effects of temperature on the structure of the alloy in the weld zone of the tube wall was discussed under Metallography. Grain growth occurred at 1725° F (1214 K) compared to no grain growth observed at 1450° F (1061 K). Carbide precipitation at the grain boundaries causes embrittlement of the structure.

The variation in the slopes of the isothermal plots of stress against equivalent strain rate shown in figure 6 (p. 14) suggests that increased creep resistance developed at higher test temperatures possibly as a result of some embrittling phase formation. Embrittling phases may be carbides or an intermetallic compound since the electron vacancy numbers indicate that this alloy may be instability prone.

In figure 5 (p. 14) strain rate data from tube test specimens has been used to obtain stress-parameter graphs for 2 and 5 percent creep deformation. These curves are based on the assumption of uniform creep, that is, the creep deformation rate of the tube specimen is constant from the beginning of life to rupture.

According to the Bailey solution, $\epsilon_{\theta} = -\epsilon_{r}$. This relation states that the circumferential strain rate is equal to, and of opposite sign to the radial strain rate. Thus, as the inside diameter grows, the pressure load in the walls increases, and the wall gets

thinner as a result of the radial strain. In the case of a ductile tube, considerable expansion and high creep strains may occur toward the end of life. The increase in the inside diameter of the tube results in higher stresses in the tube wall. This behavior is somewhat similar to the stress variation in a tensile creep rupture test specimen where the reduction in area as strain ensues results in higher tensile stresses. The use of average strain rates for tube data is believed to be conservative. That is, predicted levels of strain for a given stress and time based on figure 5 (p. 14) will be greater than actual experimental strain measurements.

An example of the application of creep rupture data in the design of N-155 tubing for 10 000 hour service life is given in the appendix.

CONCLUSIONS

Creep rupture pressure tests were conducted with specimens fabricated from welded and drawn N-155 tubes having diameter-to-wall thickness D/w ratios of 5.2 and 15. Thirty-one specimens were statically pressurized with helium at constant high temperatures in an air atmosphere for long lifetimes up to 1857 hours. Twelve specimens were thermally cycled once per day from test temperature down to 400° F (478 K) and back to test temperature. Test temperatures had a range of 1450° to 1780° F (1061 to 1244 K). Test pressures varied from 450 to 1800 psi (3.1 to 12.4 MN/m^2). A Larson-Miller curve for equivalent tube stress against parameter is presented for welded N-155 tubes. The parameter was selected and the parameter constant of 17.2 was determined by a computer program. Analysis of results of tests and study of photomicrographs leads to the following conclusions.

1. Reliable predictions of creep deformation or creep rupture lifetimes of welded N-155 tubes under given temperature and stress conditions cannot be made solely on the basis of tensile data obtained from sheet specimens.

2. Conservative predictions of creep rupture lifetimes for welded N-155 tubes of varying wall thicknesses, wall ratios, temperatures, and pressures, can be determined from the Larson-Miller diagram provided.

3. Welded N-155 tubes have approximately two-thirds of the creep rupture strengths of tensile specimens tested under corresponding conditions of temperature and lifetime.

4. Thermally cycled welded N-155 tubes have approximately 10 percent lower creep rupture strengths than tubes tested at constant temperature under corresponding conditions of test temperature and lifetime.

5. Thermal cycling of welded N-155 tubes increased the average creep rates and the average ultimate creep strains compared to the corresponding data for tubes tested at constant temperature under similar conditions.

6. Failures of welded N-155 tubing initiated on the outside of the tubes in the weld area of the tube wall. Tube walls were reduced locally in the weld area. The effective creep strain rate and the total effective strain were a maximum at the inside surface of the tube wall in the weld area.

7. Stress-strain relations from Bailey's plasticity solution for tubes under internal pressure provided a basis for the correlation of average creep strain data with stress, temperature, and the Larson-Miller parameter.

8. The creep deformation and creep rupture strength of welded N-155 tubing may be improved by metallurgically increasing the creep resistance of the weld area of the tube wall or by the production of seamless tubing.

Lewis Research Center,
National Aeronautics and Space Administration,
Cleveland, Ohio, November 26, 1968,
126-15-01-04-22.

APPENDIX - APPLICATION OF DATA

Given the following information determine the maximum operating temperature for heat exchanger tubing to be operated at constant temperature and internal pressure conditions for 10 000 hours service life.

Material, welded and drawn tubing	N-155
Tubing size:	
Diameter	0.250
Wall thickness	0.030
Pressure, psi (MN/m^2)	1500 (10.3)
Safety factor (based on creep rupture strength), N	1.50

Evaluate equation (5) at the inside radius of the tubing.

$$\bar{\sigma} = \frac{\sqrt{3}}{4.5} \frac{\left(\frac{0.125}{0.095}\right)^{2/4.5}}{\left(\frac{0.125}{0.095}\right)^{2/4.5} - 1} p = 3.36\,p = 5040 \text{ psi } (34.75 \text{ MN/m}^2)$$

Then the ultimate equivalent strength $\bar{\sigma}_u$ is obtained.

$$\bar{\sigma}_u = N\bar{\sigma} = 1.50\,(5040) = 7560 \text{ psi } (52.1 \text{ MN/m}^2)$$

From figure 5, for an equivalent stress of 7.56 ksi (52.1 MN/m^2), read the parameter value 40.50 and solve for T ^oR.

$$^oR = \frac{10^3\,P}{\log t + 17.2} = \frac{40\,500}{21.2} = 1910^o \text{ R}$$

For the conditions given, 1910^o R is the maximum operating temperature.

The stress-parameter plot for the equivalent stress (from pressure) of 5040 psi (34.75 MN/m^2) at 1910^o R for 10 000 hours falls on the 2 percent equivalent strain line in figure 5. This indicates that the equivalent strain in the bore of the tubing will be 2 percent after 10 000 hours at design conditions of temperature and pressure. The

strain at the outside diameter of the tube $\epsilon_{\theta b}$ is used to determine the expansion of the tube. $\epsilon_{\theta b}$ is obtained from equation (7).

$$\epsilon_{\theta b} = \frac{\sqrt{3}}{2}\left(\frac{a}{b}\right)^2 \bar{\epsilon}_a = \frac{0.02}{1.155 \times 1.732} = 0.01 \text{ cm/cm/}10^4 \text{ hour}$$

REFERENCES

1. Wild, John M.: Nuclear Propulsion for Aircraft. Astronautics and Aeronautics, vol. 6, no. 3, Mar. 1968, pp. 24-30.

2. Finnie, Iain: An Experimental Study of Multiaxial Creep in Tubes. Joint International Conference on Creep. Inst. Mech. Eng., 1963, pp. 2-21 to 2-26.

3. Zaslawsky, Maurice: Effect of Stress State on Flow and Fracture of Several High-Strength Alloys. Rep. UCRL-14863, Lawrence Radiation Lab., Univ. California, Apr. 27, 1966.

4. Chitty, A.; and Duval, D.: The Creep-Rupture Properties of Tubes for High Temperature Steam Power Plant. Proc. Inst. Mech. Eng., vol. 178, Pt. 3A, 1963-64

5. Manson, S. S.: Design Considerations for Long Life at Elevated Temperatures. Presented at the Joint International Conference on Creep, IME, ASTM, and ASME, London, England, Sept. 30-Oct. 4, 1963.

6. McCoy, H. E., Jr.; and Wier, J. R., Jr.: Stress-Rupture Properties of Irradiated and Unirradiated Hastelloy Tubes. Nucl. Appl., vol. 4, Feb. 1968, pp. 96-104.

7. Bailey, R. W.: Creep Relationships and Their Application to Pipes, Tubes, and Cylindrical Parts Under Internal Pressure. Proc. Inst. Mech. Eng., vol. 164, 1951, pp. 425-431.

8. Tagart, S. W., Jr.: Mechanical Design Considerations in Primary Nuclear Piping. Rep. GEAP-4578, General Electric Co., Mar. 1964.

9. Marin, Joseph: Engineering Materials: Their Mechanical Properties and Applications. Prentice-Hall, Inc., 1952.

10. Weiss, V.; and Sessler, J. G., eds.: Aerospace Structural Metals Handbook. Vol. I: Ferrous Alloys. Syracuse Univ. Press, Mar. 1963, code 1602.

11. Anon.: Multimet Alloy. Publ. No. F-30.036C, Union Carbide Stellite Co., July 1963.

12. Johnson, W.; and Mellor, P. B.: Plasticity for Mechanical Engineers. D. Van Nostrand Co., Inc., 1962, p. 350 ff.

13. Mendelson, Alexander; Roberts, Ernest, Jr.; and Manson, S. S.: Optimization of Time-Temperature Parameters for Creep and Stress Rupture, with Application to Data from German Cooperative Long-Time Creep Program. NASA TN D-2975, 1965.

14. Johnson, A. E.: Complex-Stress Creep of Metals. Met. Rev., vol. 5, no. 20, 1960, pp. 447-506.

15. Conrad, H.; Bernett, E.; and White, J.: Correlation and Interpretation of High Temperature Mechanical Properties of Certain Superalloys. Joint International Conference on Creep. Inst. Mech. Eng., 1963, pp. 1-9 to 1-15.

16. Woodyatt, L. R.; Sims, C. T.; and Beattie, H. J., Jr.: Prediction of Sigma Phase Occurrence from Compositions in Austenitic Superalloys. Trans. of the Metallurgical Society of AIME. Vol. 236, Apr. 1966, p. 519.

NASA-Langley, 1969 —— 17 E-4622

NATIONAL AERONAUTICS AND SPACE ADMINISTRATION
WASHINGTON, D. C. 20546

OFFICIAL BUSINESS

FIRST CLASS MAIL

POSTAGE AND FEES PAID
NATIONAL AERONAUTICS AND
SPACE ADMINISTRATION

"The aeronautical and space activities of the United States shall be conducted so as to contribute . . . to the expansion of human knowledge of phenomena in the atmosphere and space. The Administration shall provide for the widest practicable and appropriate dissemination of information concerning its activities and the results thereof."

—NATIONAL AERONAUTICS AND SPACE ACT OF 1958

NASA SCIENTIFIC AND TECHNICAL PUBLICATIONS

TECHNICAL REPORTS: Scientific and technical information considered important, complete, and a lasting contribution to existing knowledge.

TECHNICAL NOTES: Information less broad in scope but nevertheless of importance as a contribution to existing knowledge.

TECHNICAL MEMORANDUMS: Information receiving limited distribution because of preliminary data, security classification, or other reasons.

CONTRACTOR REPORTS: Scientific and technical information generated under a NASA contract or grant and considered an important contribution to existing knowledge.

TECHNICAL TRANSLATIONS: Information published in a foreign language considered to merit NASA distribution in English.

SPECIAL PUBLICATIONS: Information derived from or of value to NASA activities. Publications include conference proceedings, monographs, data compilations, handbooks, sourcebooks, and special bibliographies.

TECHNOLOGY UTILIZATION PUBLICATIONS: Information on technology used by NASA that may be of particular interest in commercial and other non-aerospace applications. Publications include Tech Briefs, Technology Utilization Reports and Notes, and Technology Surveys.

Details on the availability of these publications may be obtained from:

SCIENTIFIC AND TECHNICAL INFORMATION DIVISION

NATIONAL AERONAUTICS AND SPACE ADMINISTRATION

Washington, D.C. 20546